

Numerical study of the effect of the tip gap size and using a single circumferential groove on the performance of a multistage compressor

Morteza Hamzezade^a, Mohsen Agha Seyed Mirzabozorg^{a,*} and Mehrdad Bazazzadeh^a

^a Faculty of Mechanical Engineering, Malek Ashtar University of Technology, Isfahan, Iran

ARTICLE INFO

Article history:

Received: 2018-05-05

Received in revised form

Accepted

Available online

Keywords:

Circumferential groove

Multistage compressor

Tip gap

Stall margin

CFD

ABSTRACT

The effect of the tip gap size on the performance of a multistage axial compressor was studied by means of computational fluid dynamics (CFD). It was found that the performance of the compressor was very sensitive to the size of the tip gap. By increasing the gap size, the stall margin value, the total pressure ratio and the compressor efficiency reduced considerably. The flow field at the tip region of the blades at the near-stall point showed that the size of the blockage grew with an increase in the gap size. Afterward, the effect of various single circumferential grooves- having specified widths and depths at different placement positions- on the performance were investigated in the reference gap. The stall margin increased about 7% with negligible reduction of the peak efficiency using one of the grooves which placed next to the trailing edge of the first-stage rotor. Also, this groove increased the stall margin in other tip gap sizes. Investigation of the flow field of the tip region in the reference gap showed that when the groove was used, there was a reduction in the back-flow near the trailing edge of the first-stage rotor. Consequently, the stall occurred at a lower mass flow rate.

1. Introduction

The stable operation of a compressor is limited in the range of the choking, and the stall and researchers are always working to expand this range, even a slight amount. Expanding the operation range of a compressor, especially in aero-engines is very important because it eventuates in higher maneuverability. One of the most important factors that greatly affect the operation range of the compressors is the tip leakage flow. Researchers have found that the stall margin of the compressor could increase by controlling this flow. One of the methods can be used to control the tip leakage flow and to improve the stable operation range of an axial-flow compressor is the using of a casing treatment (CT). Since early 1960, various configurations such as axial slot, porous wall, and circumferential groove have been used as the casing treatment. Moore et al. [1] tested some configurations on an axial-flow rotor and found that the circumferential groove could improve the stability and the efficiency of the rotor. Prince et al. [2] conducted the first comprehensive study to understand the effective mechanism of CT but did not attain a proper understanding of it. Wenzel et al. [3] examined the effect of CT, on the performance of the 8 stage compressor J85 GE13. They

used circumferential grooves (in the first three and last three stages) and blade aligned slots (in the last three stages) separately and concluded that the use of CT does not affect the stall margin of the compressor. Azimian et al. [4] tested the effect of vaned recessed CT on a low-speed axial fan and found the coverage percentage of recess as the most important parameter. Crook et al. [5] numerically showed that the circumferential groove could delay the stall by the suction of the high blockage at the rear part of the passage and the energizing of the tip leakage flow. Fujita and Takata [6] found that the use of CT could reduce the sensitivity of the efficiency and the stall margin of the compressor to the tip gap size. Beheshti et al. [7] numerically showed that in a transonic compressor, the lower the tip gap size, the higher the pressure ratio and the stall margin. Guinet et al. [8] numerically studied the effect of a recirculating tip blowing CT on the performance of a 1.5-stage transonic compressor in different tip gaps and showed that the CT improves compressor stability at reference and increased tip gap unlike its negative effect at decreased tip gap. Some researchers (Puterbaugh et al. [9]; Furukawa et al. [10]) indicated the important role of the interaction between the tip leakage vortex and the shock wave in the transonic compressor aerodynamics. Furakawa et al. [11] showed that the vortex breakdown which occurs after the interaction between the tip leakage

* Corresponding author. Tel.: +98-21-22970212; fax: +98-21-22935341; e-mail: mirzabozorg@mut-es.ac.ir

vortex and the shock wave is one the sources of the unsteadiness in a transonic compressor. Wilke and Kau [12] used a numerical study to show that the vortex breakdown leads the compressor to the stall and the casing treatments could delay the vortex breakdown and consequently delay the stall. Ito et al. [13] expressed that circumferentially contoured casing above the blade leading edge could improve the stall margin significantly by weakening the rotating instability vortex. Vo et al. [14] proposed that the leading edge spillage and the trailing edge back-flow are two conditions necessary for triggering spike type stall, both of which are linked to the tip leakage vortex. Chen et al. [15] used unsteady simulations to show that the spike type instabilities occur when the trajectory of the tip leakage vortex becomes perpendicular to the axial direction. Legras et al. [16] investigated the effect of circumferential grooves on the vortical structure of the tip leakage. They observed that the grooves could generate a set of secondary vortices in addition to the change of the trajectory of the tip leakage vortex. Kroeckel et al. [17] tested a multistage casing treatment in a 2.5-stage axial compressor and confirmed its capability to push the surge line towards lower mass flows with negligible reduction of the peak efficiency. Kim et al. [18] numerically showed that the casing groove combined with injection could improve both of the stall margin and the peak efficiency of a transonic compressor. Taghavi and Eslami [19] used large eddy simulation to show that casing treatment reduces the amplitude of unsteadiness of tip leakage flow and gets its frequency closer to the blade passing frequency that leads a reduction of blockage and losses as a result. Kim et al. [20] optimized the configuration of the five circumferential grooves based on the steady-state simulations. Also, they studied the effect of the shape and the number of the circumferential groove on the stall margin improvement [21, 22]. Sakuma et al. [23] investigated the effect of the location and the depth of a single circumferential groove on the stability of a transonic rotor using numerical simulations. They showed the deeper the groove, the more the stability enhancement. Zhou et al. [24] numerically analyzed the distributions of axial shear stress and axial momentum flux near the tip region at the smooth and the grooved casing. They studied the effectiveness of grooves at the subsonic and supersonic tip speeds of the rotor and indicated that the grooves could improve the stall margin at only supersonic tip speed by suppressing the boundary layer separation zone. Mirzabozorg et al. [25] numerically showed the benefits of a single shallow groove to improve the stable range of a transonic compressor by suppressing the vortex breakdown and the blade suction side separation. They indicated that the best location of the groove depends on the groove width.

Despite all the studies that have been carried out until now, it must be considered that each compressor has a unique characteristic and using the same CT at different compressors could produce different results.

This paper aims to understand the effect of the tip gap size on the performance of a multistage compressor and improve its stability at different tip gap sizes by using a single circumferential groove CT. The compressor with the reference tip gap size was simulated with various grooves, and the results were compared to the simulation of it with the smooth casing. Then one of the grooves was selected due to the maximum stall margin improvement, and the compressor was simulated at different tip gap sizes with the selected groove. The flow structure near the tip of the grooved casing was compared to the smooth casing in the reference tip gap size to evaluate the effects of the selected groove on the flow field. In comparison to the author's previous work [25], the effect of a single circumferential groove on the flow field and the stability was studied in a multistage

compressor at various tip gap sizes instead of the isolated rotor at the nominal tip gap size.

1. Five-stage Compressor Geometry

The studied compressor has been designed at the transonic regime at the flight Mach number of 2. The blades have double circular arc profile. The reference tip gap is 0.3 mm for all rotors, and the stators have no gap. At the inlet of the compressor, three struts with NACA0020 profile have been used. The design specifications of the compressor are summarized in table 1, and table 2 shows the number of blades of each stage. The meridional view of the five-stage compressor has been shown in Fig. 1.

Table 1. Characteristics of the 5-stage compressor at the design point.

mass flow rate [kg/s]	2.87
total pressure ratio	3.25
isentropic efficiency	0.83
rotational speed [rpm]	35000

Table 2. Number of blades of each stage

	rotor	Stator
1 st stage	23	27
2 nd stage	31	36
3 rd stage	40	45
4 th stage	51	58
5 th stage	63	70

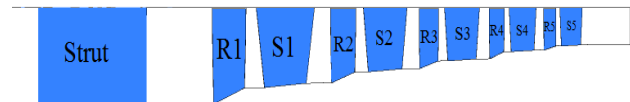


Figure 1. Meridional view of the five-stage compressor

2. Geometry of Circumferential Grooves

The schematic view of the circumferential groove has been shown in Figure 2. In this figure, d , w , C_x and x indicate the groove depth, the groove width, blade tip axial chord and the groove axial location respectively. It was assumed that the groove must be located only above the first-stage rotor between its leading edge and trailing edge. The reference tip gap size was used to normalize the depth of the groove. Also, the axial location of the groove and its width were normalized by the tip axial chord of the first-stage rotor as follows:

$$\begin{cases} d^* = \frac{d}{g} \\ w^* = \frac{w}{C_x} \times 100 \\ x^* = \frac{x}{C_x} \times 100 \end{cases} \quad (1)$$

In this paper, nineteen configurations were simulated in two types:

1. grooves with $w^* = 10$ and $d^* = 12$
2. grooves with $w^* = 20$ and $d^* = 3$

The specifications of the groove have been presented in table 3. Each configuration is distinguished by the combination of three non-dimensional numbers, which specifies as x , w and d . For example, a groove with $x^* = 30$, $w^* = 10$ and $d^* = 12$ is named "Config-x30w10d12".

Table 3. Studied configurations

x^*	w^*, d^*
0, 10, 20, 30, 40, 50, 60, 70, 80, 90	$w^* = 10, d^* = 12$
0, 10, 20, 30, 40, 50, 60, 70, 80	$w^* = 20, d^* = 3$

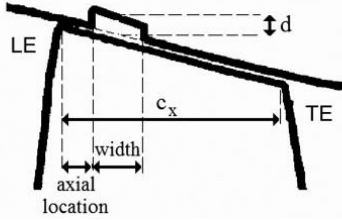


Figure 2. Schematic of circumferential groove

3. NUMERICAL ANALYSIS METHOD

3.1. Numerical Scheme

ANSYS CFX, the three-dimensional commercial solver code was utilized to solve the Reynolds-averaged Navier-Stokes (RANS) equations. To capture the flow near the walls accurately, the two-equation $k-\omega$ SST turbulence model was used. This model is the combination of the $k-\omega$ model near the walls and the $k-\epsilon$ model away from the walls. In addition to the turbulence model, an automatic wall treatment was applied to softly switch from a classical low-Reynolds formulation to logarithmic wall function according to the wall grid density [26, 27]. This automatic switch could reduce the strict grid resolution required for standard low-Reynolds formulation. All the walls were assumed to be smooth and adiabatic. In order to save the cost of the simulations, a single-passage, steady analysis was used both with and without the groove. It is based on the assumption that the flow is identical within all the blade passages. Also in the interface between the rotor and the stator, it was assumed that the non-uniform flow upstream of the interface is mixed out so that it becomes pitchwise, but not spanwise, uniform downstream of it (mixing plane method). The rotor-to-stator axial gap has not been considered in the simulations and the flow was considered to be fully turbulent. The interface between the rotor domain and the groove (Figure 3) is an unmatched interface and the general grid interface (GGI) method was used for it. The uniform total pressure, total temperature, and the flow angle were utilized as the inlet boundary condition. The hub static pressure with the radial equilibrium was used as the outlet boundary. In this set of boundary conditions, the compressor mass flow is explicitly calculated.

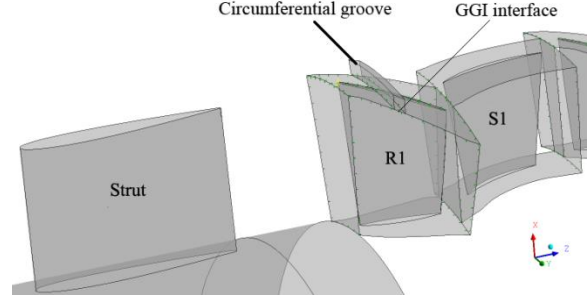


Figure 3. The GGI interface between the circumferential groove and the blade passage

The convergence criteria were considered to reach the defined residual values with the stable important parameters such as the mass flow rate and the total pressure ratio. The near-stall point of the compressor was found by tracking the iteration history of the mass flow and the total pressure ratio. The near-stall point was defined as the lowest possible mass flow that led to a converged stable solution. After the near-stall point a continuous reduction of the mass flow and the pressure ratio comes to pass when the iteration count increases known as the numerical stall. This approach of finding the near-stalling mass flow using steady RANS solutions has been applied by many researchers such as Sakuma et al. [23]. However, steady RANS solutions are limited until the near-stall point and could not model the stall properly because of inherently unsteady physics of it.

The compressor has been designed for the sea level flight condition, but all simulations have been carried out at the sea level static condition. The corrected speed of these two conditions must be the same in order to be equivalent to each other [28] as follows:

$$\frac{N_{static}}{\sqrt{T_{0static}}} = \frac{N_{flight}}{\sqrt{T_{0flight}}} \quad (2)$$

N and T_0 represent the rotational speed and the inlet total temperature, respectively. Also, the subscripts static and flight refer to the sea level static condition and sea level flight condition, respectively. According to the equation 2, N_{static} is equal to 32725 rpm.

3.2. Computational grid

The effect of the computational grid size on the simulation was studied by creating three structured mesh with O-grid topology near the blade and H/J/C/L topology in far of the blade. The characteristic maps of the compressor achieved by three computational grids have been plotted against normalized mass flow rate (\dot{m}/\dot{m}_{choke}) in Figure 4. It indicates only slight changes in the total pressure ratio, the adiabatic efficiency and the near-stall point mass flow rate when the grid size enlarges from 2471556 to 4840731 nodes. Therefore, the grid with 2471556 nodes was chosen. In the chosen grid, for instance, the first-stage rotor has 64 streamwise, 67 circumferential and 65 spanwise nodes and the tip gap has 15 spanwise nodes. A similar topology was used in all other passages. The minimum distance of nodes from the wall was considered to be 1×10^{-6} (m) to reach $y^+ < 2$.

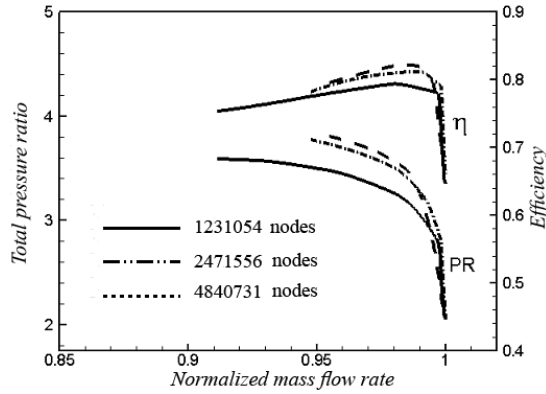


Figure 4. Grid study on characteristic maps of five-stage compressor

Also, a structured grid was used in the groove domain. The grooves of type A consist of 41 streamwise, 61 circumferential and 61 spanwise nodes and the grooves of type B consist of 51 streamwise, 61 circumferential and 31 spanwise nodes. The computational grid of the first-stage rotor has been shown in figure 5.

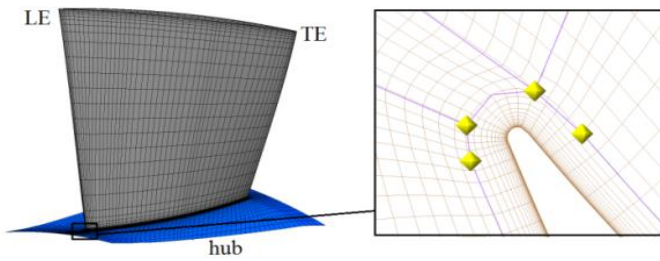


Figure 5. Computational grid of 1st stage rotor

3.3. Validation

To validate numerical scheme, NASA rotor 37- a well-known transonic compressor- was simulated and the results were verified with the experimental measurements [29]. The data of NASA rotor 37 is presented in table 4. The total pressure ratio is 2.106, and the mass flow rate is 20.19 kg/s at the design point. The rotor chokes on 20.93 kg/s and stalls at 0.925 of the choked mass flow. At the design speed (17,188.7 rpm), the measured size of the tip gap is 0.356 mm, and the relative Mach number at the inlet is 1.48 and 1.13 at the tip and the hub, respectively.

Table 4. Design specifications of NASA Rotor 37 [29]

Blade Number	36
Blade profile	Multiple Circular Arc
Blade tip radius (mm)	252
Blade tip speed (m/s)	454
Hub-tip ratio	0.7
Aspect ratio	1.19
Solidity at tip	1.288

The details of the grid study and the simulation have been described in the author's previous paper [25]. According to the paper, the selected grid of rotor 37 consists of 471154 nodes with 99 streamwise, 59 circumferential and 79 spanwise points and the tip gap has 15 spanwise nodes.

Calculated radial distribution of the total pressure ratio and the total temperature ratio at station 4 (Figure 6) were plotted against the experimental one at near the peak efficiency condition (Figure 7). The proper similarity is seen between the numerical and the experimental data. As regards the gap between the rotor hub and the stationary hub was not considered, there is a mismatch between the calculated and the measured data near the hub. Similar observations have been reported by others [29].

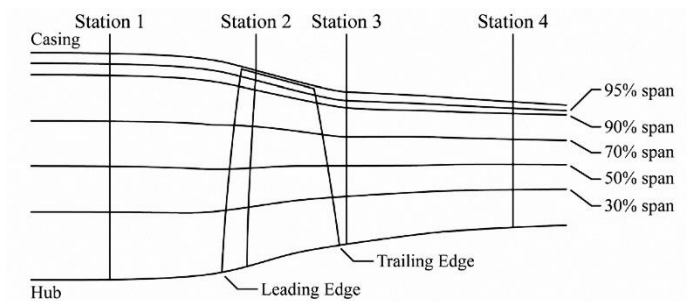


Figure 6. Measurement locations of NASA rotor 37 [29]

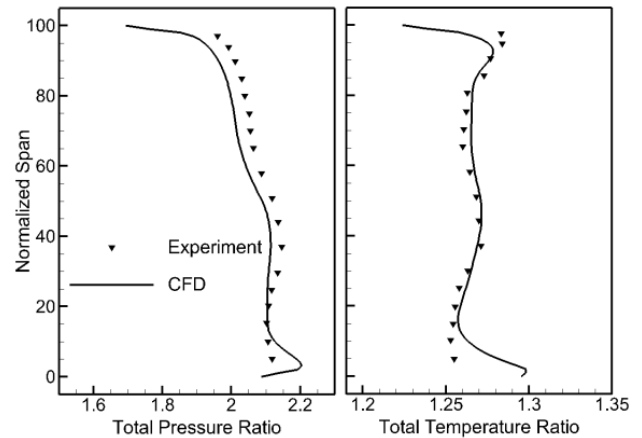


Figure 7. Spanwise distribution of the total pressure ratio and the total temperature ratio at the station 4 of NASA rotor 37 [25]

Also, the calculated characteristic maps of the rotor have been compared with the test data at the design speed in Figure 8. In the figure, uniform underestimations of the total pressure ratio and the adiabatic efficiency can be seen through the entire range of operation with the similar trend of the experimental data. The simulation predicts the near-stall point to be 0.913 of the choked mass flow which is 0.012 lower than the measured one. However, the simulation has proper reliability to predict the flow field and the performance of the compressor.

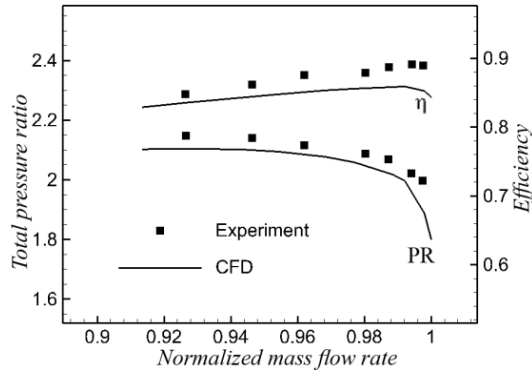


Figure 8. Characteristic maps of NASA rotor 37 [25]

4. RESULTS AND DISCUSSION

4.1. Effect of tip gap size on the five-stage compressor performance

In the design process, the reference tip gap size is intended to be 0.3 mm for all the rotors. Also, the compressor was simulated with two other tip gap sizes (half and twice of the reference) to investigate the effect of its size on the performance. The map of the compressor has been shown in Figure 9 that indicates high sensitivity to the tip gap size. According to this figure, when the gap size increases, the efficiency and the total pressure ratio of the compressor decrease at the entire operation range. Furthermore, the stable range of the compressor decreases considerably with reduction of the choke flow rate and the increase of the stall flow rate.

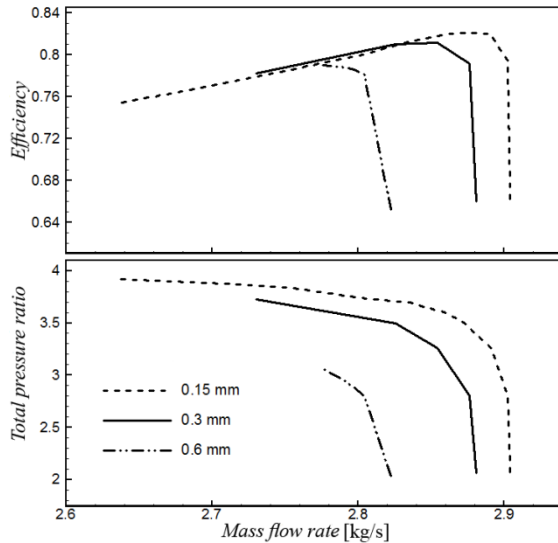


Figure 9. Effect of the tip gap size on the characteristic map of the five-stage compressor

Figure 10 shows the negative axial velocity regions at span 98% that illustrate the reversed flow and blockage in the whole domain. It can be seen that the regions of negative axial velocity have grown circumferentially with increasing the gap size. Also, Figure 11 shows

radial growth of these regions through the first-stage rotor. The increased gap size leads to more blockage and less energy transfer from the blade to the fluid and accordingly lower the total pressure ratio and the efficiency. Furthermore, Figure 12 illustrates the stronger interaction between the tip leakage vortex and the shock wave at larger tip gaps that imposes the deformation of the shock wave and creation of the low momentum region behind the shock wave.

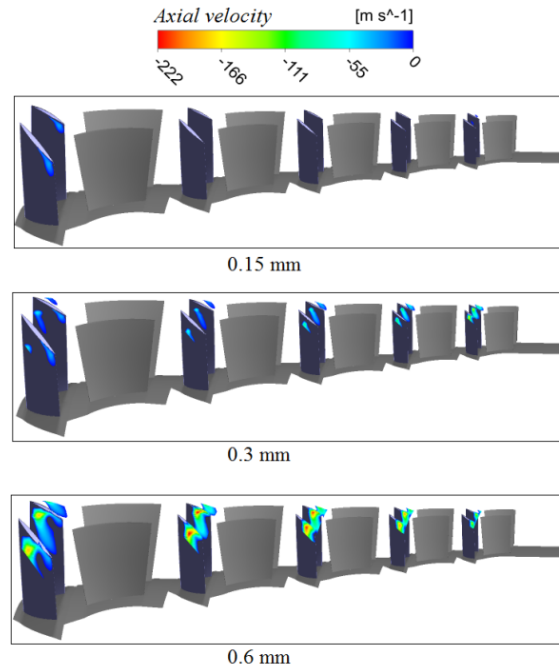


Figure 10. Negative axial velocity regions at span 98% in different tip gap sizes

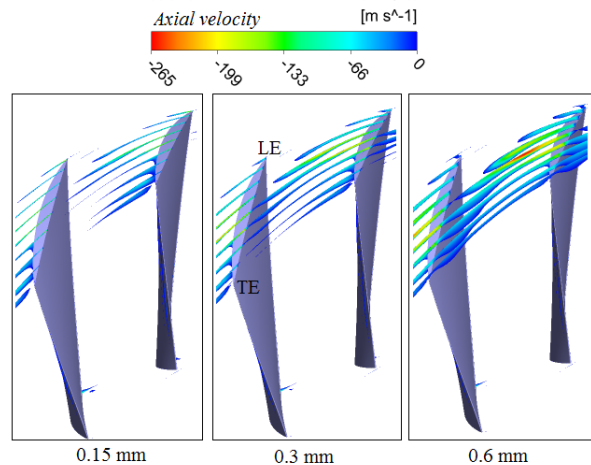


Figure 11. Negative axial velocity regions at the tip region of the first stage rotor, $m=2.8$ kg/s

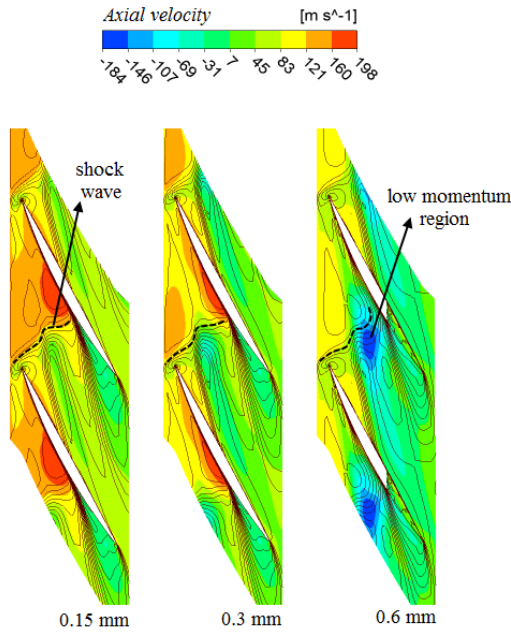


Figure 12. Effect of the tip gap size on the axial velocity in the first-stage rotor at 98% of span and superimposed relative Mach number isolines, $\dot{m}=2.8$ kg/s

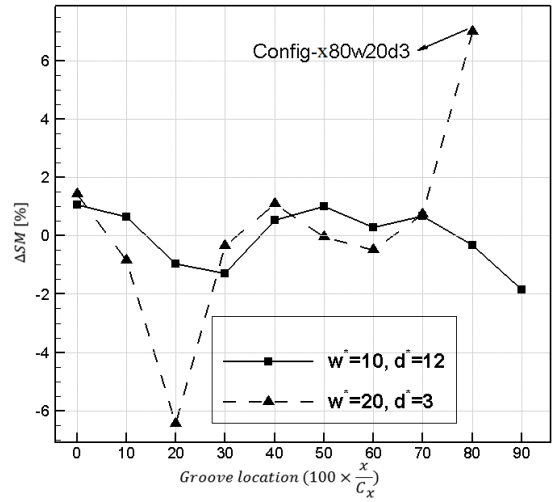


Figure 13. Effect of various circumferential grooves on the stall margin improvement of five-stage compressor

Figure 14 shows that some of the grooves increase the peak efficiency of the compressor over 0.2 percent, and the rest of the grooves have a little effect on it. Since the Config-x80w20d3 has the maximum stall margin improvement with a little effect on the peak efficiency, this groove was selected as the optimal groove.

4.2. Effect of various circumferential grooves on the five-stage compressor performance with the reference tip gap size

In this part of the paper, the effects of the grooves on the stall margin and the maximum efficiency of the compressor have been investigated. The value of the stall margin of an axial-flow compressor is calculated as below [20]:

$$SM = \left(\frac{\dot{m}_{peak}}{\dot{m}_{stall}} \times \frac{PR_{stall}}{PR_{peak}} - 1 \right) \times 100 \% \quad (3)$$

The stall margin of the studied compressor with smooth casing was calculated 19.045%. The improvement of the stall margin and the peak efficiency are evaluated as follow:

$$\Delta SM = SM_{GC} - SM_{SC} \quad (4)$$

$$\Delta \eta_{peak} = \eta_{peak_{GC}} - \eta_{peak_{SC}} \quad (5)$$

Figure 13 shows the effect of various grooves on the stall margin improvement of the compressor in the reference tip gap size. It shows that most configurations affect the stall margin less than 2%, about half of them positive and half negative. Only two configurations have a significant effect: Config-x20w20d3 decreases the stall margin by 6.44%, while Config-x80w20d3 increases it about 7%. Unlike some studies [23] that have reported the small effect of using the groove next to the blade trailing edge, Config-x80w20d3 has the maximum stall margin improvement despite locating next to the blade trailing edge.

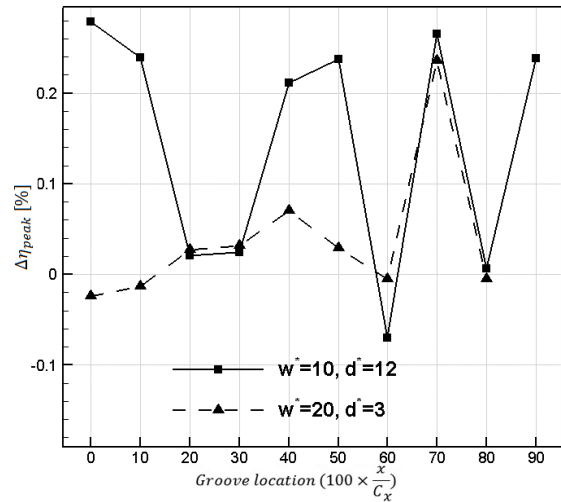


Figure 14. Effect of various circumferential grooves on the maximum efficiency of the compressor

4.3. Effect of the Config-x80w20d3 on the compressor characteristic map at various tip gap sizes

As mentioned before, Config-x80w20d3 increased the stall margin of the compressor in the reference gap. This groove was used at two other tip gap sizes, 0.15 mm and 0.6 mm, respectively half and twice of the reference value. Figure 15 shows the characteristic maps of the compressor at three gap values with and without the groove. It reveals that using the groove could improve the stall margin considerably at all gap sizes. Furthermore, it increases the total pressure ratio and the efficiency at the large gap. The value of

the stall margin improvement at three gap sizes is provided in table 5. It shows the larger the gap, the more the improvement attains in the stall margin.

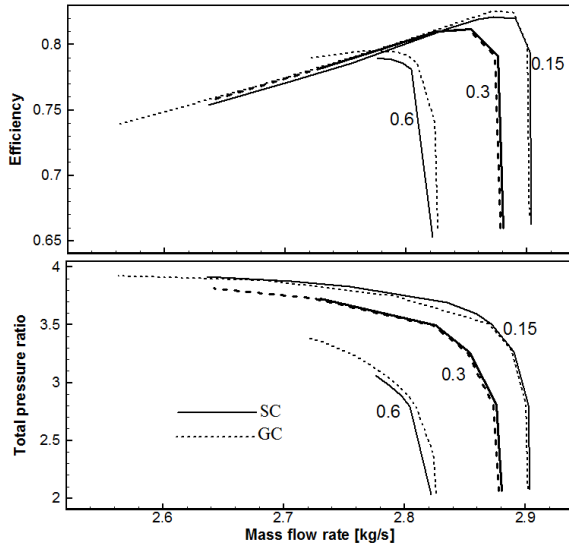


Figure 15. Effect of the Config-x80w20d3 on the characteristic map of five-stage compressor in different tip gap sizes

Table 5. Effect of the Config-x80w20d3 on the stall margin improvement of the compressor with different tip gap sizes

[mm] gap size	0.15	0.3	0.6
stall margin improvement	3.74%	6.98%	9.87%

4.4. Effect of the Config-x80w20d3 on the flow field of the compressor with the reference tip gap size

A circumferential groove usually affects the flow near the tip region. To better understanding its effects, the tip region flow of the first-stage rotor of the smooth casing is compared to the grooved one. The comparison was done at the near-stall point of the smooth casing with the reference gap. In Figure 16, the left and the middle contours represent the axial velocity in the smooth casing and axial velocity difference between the grooved casing and the smooth casing at 98% span respectively. The right contour shows the regions of negative radial velocity at the interface between the groove and the passage which indicates flow discharge from the groove to the passage. This discharge of the flow imposes an increase in the axial velocity near the blade trailing edge (middle contour). The initiation of back-flow at the trailing edge plane was represented as one of the factors that could lead to the stall by Vo et al. [14]. At the studied compressor, using circumferential groove next to the trailing edge could delay the stall by attenuation of the back-flow which has been marked in Figure 17.

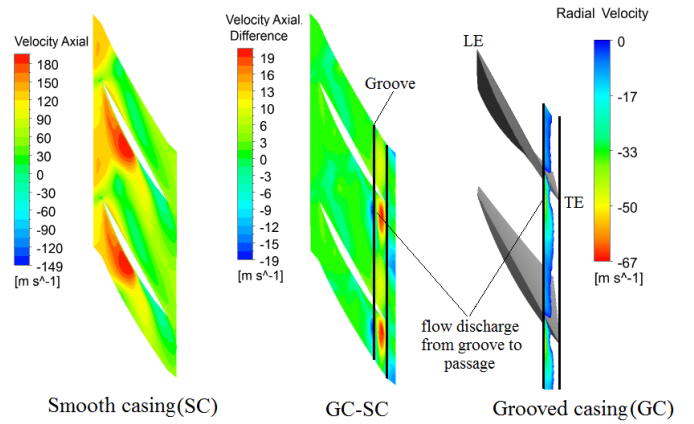


Figure 16. Effect of the Config-x80w20d3 on the flow field of the first-stage rotor (left: axial velocity contour at 98% span (SC) - center: difference of the axial velocity at 98% span (GC-SC) - right: contour of the radial velocity at the interface between the groove and the passage)

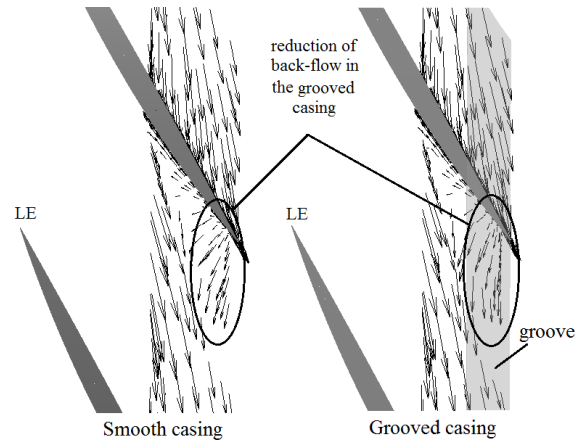


Figure 17. Projection of velocity vectors at span 98% of the first-stage rotor

Figure 18 compares the trajectories of the tip leakage flow of the grooved casing with the smooth casing at the near-stall point of the smooth casing. The streamlines are divided into two categories which are distinguished in the figure with gray and black lines. The gray streamlines originate from the tip gap between the blade leading edge and the groove leading edge (0-80% of the tip axial chord) and the black streamlines originate from the tip gap between the groove leading edge and the groove trailing edge (80-100% of the tip axial chord). In other words, the black streamlines start from the 20% of the blade rear part where the groove has been located. In the smooth casing, the black streamlines extend into the upstream and enlarge the tip leakage vortex by rolling around it. According to the figure, the groove has controlled the streamlines originating from the tip gap near the blade trailing edge and has prevented most of them from rolling around the tip leakage vortex.

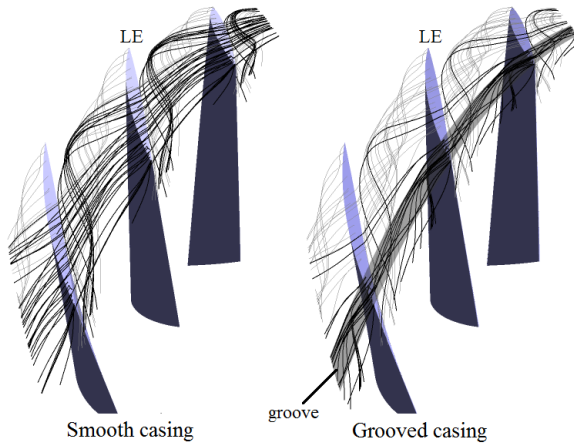


Figure 18. Effect of the Config-x80w20d3 on the tip leakage flow of the first-stage rotor

5. CONCLUSION

Steady RANS simulations were employed to study the effect of a single circumferential groove casing treatment on the flow and the stability of a five-stage compressor. The conclusions are summarized as follows:

1. The operation range of the studied compressor is very sensitive to the gap size so that when the gap size increases, the choke flow rate decreases, and the stall flow rate increases significantly.
2. When the gap size increases, a considerable reduction in the total pressure ratio and the adiabatic efficiency is seen. Also, the blockage near the tip region grows due to the enlargement of the tip leakage vortex.
3. Only one of the nineteen studied grooves give us the proper improvement of the stall margin with a slight effect on the peak efficiency.
4. This particular groove (Config-x80w20d3) covers 20% of the blade rear part. It increases the stall margin at various tip gap sizes, so the maximum improvement is achieved at a minimum gap size.
5. The flow discharge from the groove to the passage imposes an increase in the axial velocity near the blade trailing edge; consequently, the attenuation of the back-flow and the delay of the stall occur.
6. The groove controls the streamlines originating from the tip gap near the blade trailing edge and prevents most of them from rolling around the tip leakage vortex.
7. Finally, using the single circumferential groove at the first-stage rotor of the multistage compressor displays a proper capacity for improving its stability by effecting a change in the tip flow near the blade trailing edge.

6. Acknowledgment

Our gratitude is expressed to the staff of High Performance Computing Center of the Malek Ashtar University of Technology.

7. FUNDING

The authors disclose that the research was supported by the Institute of Engine and Propulsion of the Malek Ashtar University of Technology.

8. List of symbols

CFD	computational fluid dynamics
CT	casing treatment
C_x	axial tip chord [mm]
d	depth of groove [mm]
g	tip gap size [mm]
LE	leading edge of blade
\dot{m}	mass flow rate [kg/s]
N	rotational speed [rpm]
PR	total pressure ratio
SM	stall margin
TE	trailing edge of blade
T_0	total temperature
x	axial location of the groove
w	width of the groove [mm]
y^+	non-dimensional wall distance
ΔSM	stall margin improvement
$\Delta \eta_{peak}$	variation in peak efficiency
η	adiabatic efficiency
Subscripts and superscripts	
flight	flight condition
GC	grooved casing
peak	peak adiabatic efficiency point
SC	Smooth casing
stall	near-stall point
*	non-dimensional number
static	static condition

9. References

- [1] R. D. Moore, G. Kovich, R. J. Blade, Effect of casing treatment on overall and blade element performance of a compressor rotor, 1971.
- [2] D. Prince, D. Wisler, D. Hilvers, A study of casing treatment stall margin improvement phenomena, in Proceeding of, American Society of Mechanical Engineers, pp. V01AT01A059-V01AT01A059.

- [3] L. M. Wenzel, J. E. Moss, C. M. Mehalic, 1975, Effect of casing treatment on performance of a multistage compressor, National Aeronautics and Space Administration,
- [4] A. Azimian, R. Elder, A. McKenzie, Application of recess vaned casing treatment to axial flow fans, *Journal of Turbomachinery*, Vol. 112, No. 1, pp. 145-150, 1990.
- [5] A. Crook, E. M. Greitzer, C. Tan, J. Adamczyk, Numerical simulation of compressor endwall and casing treatment flow phenomena, *Journal of turbomachinery*, Vol. 115, No. 3, pp. 501-512, 1993.
- [6] H. Fujita, H. TAKATA, A study on configurations of casing treatment for axial flow compressors, *Bulletin of JSME*, Vol. 27, No. 230, pp. 1675-1681, 1984.
- [7] B. H. Beheshti, J. A. Teixeira, P. C. Ivey, K. Ghorbanian, B. Farhanieh, Parametric study of tip clearance-casing treatment on performance and stability of a transonic axial compressor, in *Proceeding of, American Society of Mechanical Engineers*, pp. 395-404.
- [8] C. Guinet, J. A. Streit, H.-P. Kau, V. Gümmer, Tip gap variation on a transonic rotor in the presence of tip blowing, in *Proceeding of, American Society of Mechanical Engineers*, pp. V02AT37A002-V02AT37A002.
- [9] S. Puterbaugh, M. Brendel, Tip clearance flow-shock interaction in a transonic compressor rotor, *Journal of propulsion and power*, Vol. 13, No. 1, pp. 24-30, 1997.
- [10] M. Furukawa, M. Inoue, K. Saiki, K. Yamada, The role of tip leakage vortex breakdown in compressor rotor aerodynamics, in *Proceeding of, American Society of Mechanical Engineers*, pp. V001T01A054-V001T01A054.
- [11] M. Furukawa, K. Saiki, K. Yamada, M. Inoue, Unsteady flow behavior due to breakdown of tip leakage vortex in an axial compressor rotor at near-stall condition, in *Proceeding of, American Society of Mechanical Engineers*, pp. V001T03A112-V001T03A112.
- [12] I. Wilke, H.-P. Kau, A numerical investigation of the influence of casing treatments on the tip leakage flow in a HPC front stage, in *Proceeding of, American Society of Mechanical Engineers*, pp. 1155-1165.
- [13] Y. Ito, T. Watanabe, T. Himeno, Effects of endwall contouring on flow instability of transonic compressor, *Int. J. Gas Turb. Propul. Power Sys*, Vol. 2, No. 1, pp. 24-29, 2008.
- [14] H. D. Vo, C. S. Tan, E. M. Greitzer, Criteria for spike initiated rotating stall, *Journal of turbomachinery*, Vol. 130, No. 1, pp. 011023, 2008.
- [15] J.-P. Chen, M. D. Hathaway, G. P. Herrick, Prestall behavior of a transonic axial compressor stage via time-accurate numerical simulation, *Journal of Turbomachinery*, Vol. 130, No. 4, pp. 041014, 2008.
- [16] G. Legras, N. Gourdain, I. Trebinjac, Numerical analysis of the tip leakage flow field in a transonic axial compressor with circumferential casing treatment, *Journal of Thermal Science*, Vol. 19, No. 3, pp. 198-205, 2010.
- [17] T. Kroeckel, S. Hiller, P. Jeschke, Application of a multistage casing treatment in a high speed axial compressor test rig, in *Proceeding of, American Society of Mechanical Engineers*, pp. 309-318.
- [18] D.-W. Kim, J.-H. Kim, K.-Y. Kim, Aerodynamic performance of an axial compressor with a casing groove combined with injection, *Transactions of the Canadian Society for Mechanical Engineering*, Vol. 37, No. 3, pp. 283-292, 2013.
- [19] R. Taghavi-Zenouz, S. Eslami, Effects of casing treatment on behavior of tip leakage flow in an isolated axial compressor rotor blade row, *Journal of the Chinese Institute of Engineers*, Vol. 36, No. 7, pp. 819-830, 2013.
- [20] J.-H. Kim, K.-J. Choi, K.-Y. Kim, Aerodynamic analysis and optimization of a transonic axial compressor with casing grooves to improve operating stability, *Aerospace Science and Technology*, Vol. 29, No. 1, pp. 81-91, 2013.
- [21] J. Kim, K. Choi, K. Kim, Performance evaluation of a transonic axial compressor with circumferential casing grooves, *Proceedings of the Institution of Mechanical Engineers, Part A: Journal of Power and Energy*, Vol. 226, No. 2, pp. 218-230, 2012.
- [22] J. H. Kim, K. Y. Kim, K. H. Cha, Effects of number of circumferential casing grooves on stall flow characteristics of a transonic axial compressor, in *Proceeding of, Trans Tech Publ*, pp. 727-732.
- [23] Y. Sakuma, T. Watanabe, T. Himeno, D. Kato, T. Murooka, Y. Shuto, Numerical analysis of flow in a transonic compressor with a single circumferential casing groove: influence of groove location and depth on flow instability, *Journal of Turbomachinery*, Vol. 136, No. 3, pp. 031017, 2014.
- [24] X. Zhou, Q. Zhao, X. Xiang, W. Cui, Investigation of groove casing treatment in a transonic compressor at different speeds with control volume method, *Proceedings of the Institution of Mechanical Engineers, Part G: Journal of Aerospace Engineering*, Vol. 230, No. 13, pp. 2392-2408, 2016.
- [25] M. A. S. Mirzabozorg, M. Bazazzadeh, M. Hamzezade, Numerical study on the effect of single shallow circumferential groove casing treatment on the flow field and the stability of a transonic compressor, *Journal of Applied Fluid Mechanics*, Vol. 10, No. 1, pp. 257-265, 2017.
- [26] F. Menter, J. C. Ferreira, T. Esch, B. Konno, A. Germany, The SST turbulence model with improved wall treatment for heat transfer predictions in gas turbines, in *Proceeding of, 2-7*.
- [27] F. R. Menter, Review of the shear-stress transport turbulence model experience from an industrial perspective, *International Journal of Computational Fluid Dynamics*, Vol. 23, No. 4, pp. 305-316, 2009.
- [28] S. L. Dixon, C. Hall, 2010, *Fluid mechanics and thermodynamics of turbomachinery*, Butterworth-Heinemann,
- [29] J. Dunham, CFD validation for propulsion system components (la validation CFD des organes des propulseurs), *ADVISORY GROUP FOR AEROSPACE RESEARCH AND DEVELOPMENT NEUILLY-SUR-SEINE (FRANCE)*, pp. 1998.